Wireless imaging of transient redox activity based on bipolar light-emitting electrode arrays

Gerardo Salinas, S. Mohsen Beladi-Mousavi, Liubov Gerasimova, Laurent Bouffier, Alexander Kuhn

Wireless imaging of transient redox activity based on bipolar light-emitting electrode arrays

Gerardo Salinas*, S. Mohsen Beladi-Mousavi, Liubov Gerasimova, Laurent Bouffier, Alexander Kuhn*

Univ. Bordeaux, CNRS, Bordeaux INP, ISM, UMR 5255, ENSCBP, 33607, Pessac, France.

ABSTRACT: Bipolar electrochemistry (BE) is a wireless electrochemical technique, which enables asymmetric electroactivity on the surface of conducting objects. This technique has been extensively studied for different electrochemical applications including synthesis, separation, sensing, and surface modification. Here, we employ BE for imaging the transient electrochemical activity of different redox species with high accuracy via an array of light-emitting diodes having different lengths. Such a gradient allows the differentiation of redox systems due to their intrinsic difference in thermodynamic potential and the evaluation of their diffu-sional behavior based on the intensity of light emission. The result is an instantaneous optical readout of analytical information, equivalent to classic electrochemical scanning techniques such as linear sweep voltammetry.

Electrochemical methods are powerful tools for the evalua-tion of redox activity of different species in solution.1 Bipolar electrochemistry (BE) is a particularly interesting approach due to the wireless generation of asymmetric electroactivity on the surface of a conducting object.2-5 In the simplest exper-imental configuration, a conducting object is freely positioned in an electrolyte solution between two feeder electrodes. Upon exposure to an external electric field (ε), a polarization potential difference (ΔV) is generated along the object. In the presence of electroactive species, redox reactions can occur at its both extremities, as long as ΔV exceeds the thermodynamic threshold potential required to trigger both reactions simulta-neously (ΔVmin). Above this critical potential, the conducting object behaves as a bipolar electrode (BPE). This approach has been extensively used in electrosynthesis,6 photo-electrochemistry,7 electrochemical separation8 and electro-chemical sensing.9,10 In particular, the wireless optical imaging of redox activity is a very attractive concept.11,12 It is based on the coupling of a redox reaction of interest at one extremity of the BPE, with an optical readout produced by a chemical or electrochemical reaction, at the opposite side of the device.13-16 Redox activity at one side of a BPE has been monitored by the modulation of fluorescence intensity17,18 or electrochemi-luminescence (ECL) emission.19-21 Commonly, ECL has been used as an accurate readout of the electrochemical information of a coupled redox reaction.22,23 An interesting approach is to mimic conventional potentiodynamic current recordings by the correlation between the ECL intensity and the interfacial potential gradient across a BPE.24,25 For example, Crooks et al. obtained an optical potentiodynamic curve by using a triangu-lar-shaped BPE. The triangular configuration mimics a classic three-electrode configuration, since the larger side acts as the counter electrode and the tip as the working electrode. Such a geometry ensures that the rate of the ECL reaction is not limited by the corresponding reduction, leading in fine to electrochemical information similar to the one obtained by conventional potential sweeping methods.24 Anand et al. generated similar optical potentiodynamic curves by using an array of closed BPEs. In this case, the overall interfacial po-tential gradient is controlled by the distance between each BPE and the feeder electrodes.25

Scheme 1. Illustration of the bipolar light-emitting elec-trode array with a representation of the associated chemi-cal reactions.

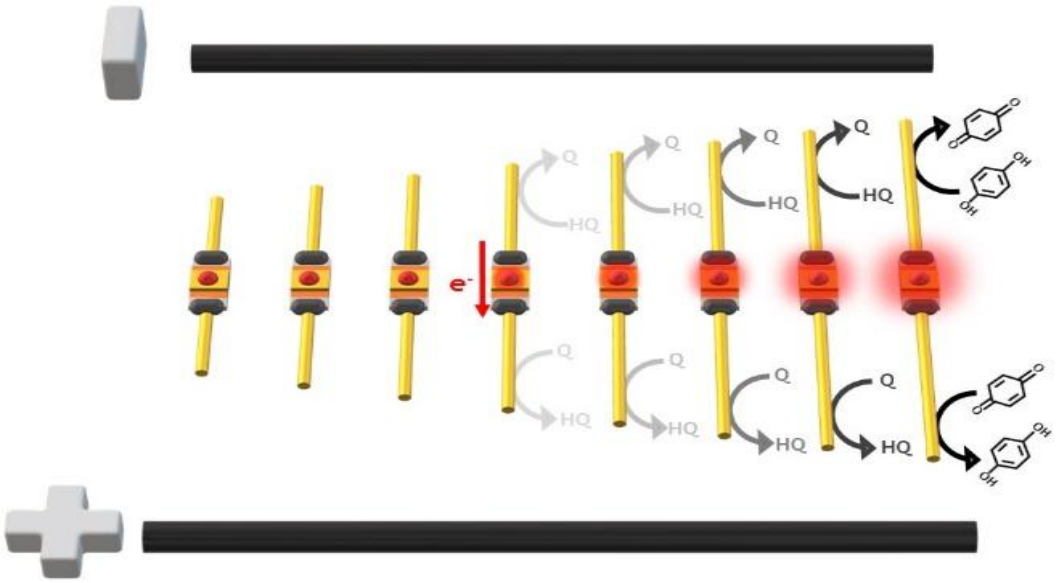

Apart from ECL, a promising alternative is the use of light-emitting diodes (LEDs) for the direct visualization of bipolar electrochemical reactions. In such devices, light emission can be triggered either by coupling thermodynamically spontane-ous reactions to the terminals of the LED26,27 or by using an external electric field as a driving force.28-32 Recently, such approaches have been used for the readout of chemical infor-mation via the light emission originating from the integrated LED. These systems are based on the selective oxidation of biochemical33 or chiral probes34,35 at the anodic terminal of the LED, coupled with the reduction of protons at the cathodic side. In such devices, the analytical information is directly encoded by the electric current passing through the LED and thus also by the concomitant light emission. Herein, we take advantage of such a light-emitting device to design a light-emitting bipolar array, which allows imaging the redox activi-ty of electroactive species via a gradient of BPEs with differ-ent lengths (Scheme 1). Considering that the maximum polari-zation potential difference for a given electric field value, is proportional to the length of the BPE, a gradual change in the length of the object produces a gradient of ΔV along the array. Thus, under these conditions, only the BPEs with a ΔV above the thermodynamic threshold potential can emit light. The major advantage with respect to the other optical BE readout approaches reported in the literature so far, essentially based on ECL, is that no other chemical ingredients such as a lumi-nophore and an ECL co-reactant are necessary. This potential-ly avoids any parasitic reactions with the analyte, when the detection scheme is for example based on the use of DNA or enzymes.

The light-emitting bipolar array was assembled by connect-ing a gold wire to the anode and the cathode of each LED. In brief, thirty-seven LEDs, with 1 mm spacing between them, and their corresponding Au electrodes were immobilized on a glass plate. Of course, the number of LEDs can be adjusted if necessary. The electrodes and the LEDs were connected using electrically conductive silver paste. Afterwards, each BPE was cut to the desired length (between 1 and 2.08 cm, Figure 1a), and their theoretical polarization potential difference (ΔVtheo) was calculated for different electric field values (Fig-ure S1). Considering the intrinsic threshold potential of the used LED (1.55 V), electric field values below 0.75 V/cm do not provide enough driving force to switch on any of the BPEs. When the applied electric field is gradually increased, ΔVtheo allows switching on exclusively the LEDs having the appropriate length. The threshold potential is modulated by the difference in thermodynamic potential between the anodic and cathodic reactions. Thus, redox reactions with a relatively small peak-to-peak separation (ΔV) between the anodic and cathodic reactions require a lower driving force to switch on the LEDs. As a proof of concept, the redox couple hydroqui-none, i.e.

benzene-1,4-diol/1,4-benzoquinone (HQ/Q) was used as the initial probe, since it presents a relatively small ΔV i.e., 110 mV (Figure S2).

The light-emitting bipolar array was placed at the center of a bipolar cell, containing for the first control experiment only an aqueous 5 mM LiClO4 solution. The electrochemical re-sponse of the bipolar electrode array was monitored by video macroscopy recordings of its light emission. As stated above, an electric field above 0.75 V/cm is required for the BPE array to emit light, thus, an ε of 1.5 V/cm was applied. Under these conditions, the generated ΔV is insufficient to trigger the oxidation and reduction of water at the anodic and cathodic arms of the LEDs, respectively (Figure S3, red line). Howev-er, when the same experiment is carried out in the presence of an equimolar HQ/Q solution (5 mM), this redox probe causes a decrease in the required driving force to trigger light emis-sion (Figure S3, black line). As stated above, only the BPEs experiencing a ΔV above the thermodynamic threshold poten-tial can trigger the oxidation and reduction of HQ and Q, respectively (Scheme 1). By plotting the average light intensi-ty as a function of the BPE length, it was possible to obtain an almost sigmoidal response (Figure 1). This behavior can be considered as the analog of a potentiodynamic response ob-tained by conventional linear sweep voltammetry. For a given electric field (1.5 V/cm), BPEs having a length in the range between 1.6 and 1.9 cm show the characteristic exponential increase in signal, associated with the charge transfer limited kinetics (Butler-Volmer regime, Figure 1, pink region). For BPEs with a length above 1.9 cm, the driving force becomes so strong that light emission is governed by mass transport limitations (Figure 1, green region). Theoretically, this de-crease of light intensity might be also related to a possible passivation of the electrodes, in particular when using the HQ/Q redox probes. However, a similar decay of light intensi-ty as a function of time is also observed when using the Fe(CN)64–/Fe(CN)63– redox couple. This leads us to the con-clusion that the decrease of light intensity is the result of the local depletion of analyte.

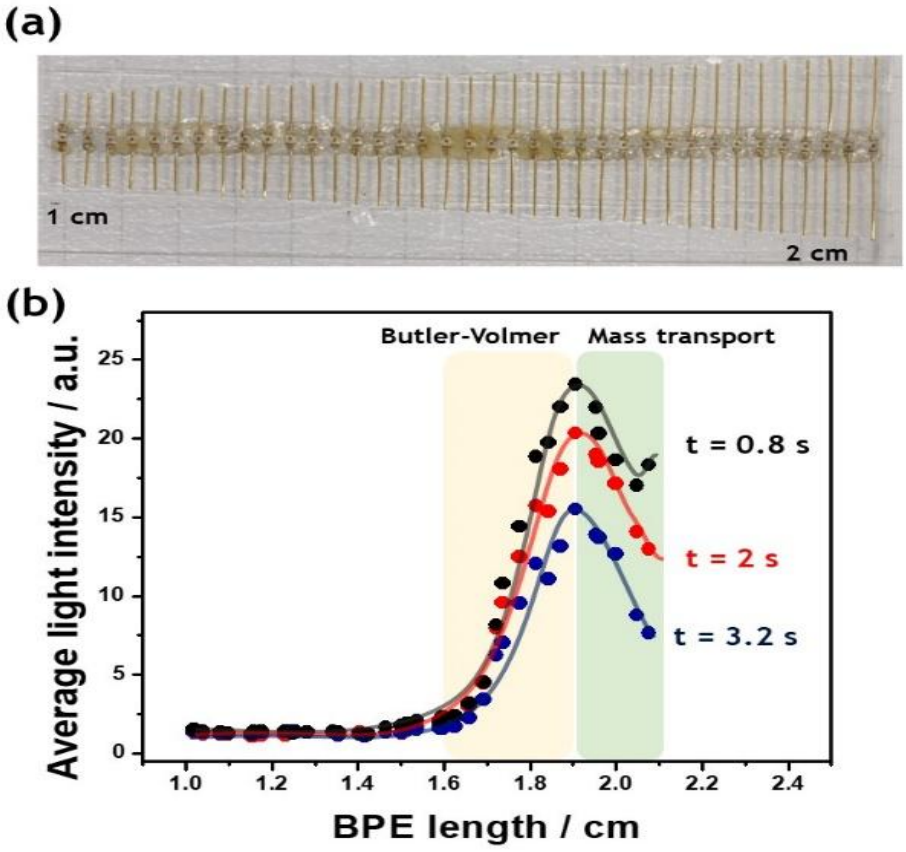

Figure 1. (a) Photograph of the bipolar electrode array. (b) Average of the light intensity distribution as a function of the BPE length obtained in a 5 mM LiClO4 solution in the presence of a 1:1 ratio of Hydroquinone/Quinone solution (HQ/Q, 5:5 mM) at a constant global electric field (1.5 V/cm) and for three different times (indicated in the plot). The average of the rela-tive standard deviation obtained from three independent exper-iments is ±10-15%.

Due to the configuration of the array, it is possible to con-sider each BPE as an individual electrochemical measurement system. Thus, plotting the maximum light intensity as a func-tion of time allows evaluating the diffusional behavior (Figure 2). Such plots for two different BPEs (1.69 and 1.91 cm in length) show transients analog to chronoamperometric meas-urements in classic potentiostatic experiments (Figure S4). It can be noticed, as expected, that for the longer bipolar elec-trode the optical signal decays faster due to a higher driving force. However, further analysis by plotting the maximum light intensity as a function of 1/t1/2, indicate that the light emission transients do not follow a Cottrell like behavior (Inset Figure S4). Theoretically, due to the geometry of each extremity of the BPE, mass transport occurs according to a cylindrical diffusion profile. For this case, the current is a function of the dimensionless parameter $\tau = 4Dt/r2$, where D is the diffusion coefficient and r is the radius of the elec-trode.1 In the short-time limit when τ is considerably small, current follows a Cottrell behavior.36 Nonetheless, deviations from the characteristic Cottrell profile start when τ reaches a value around 0.01. Thus, in the frame of this work, cylindrical diffusion is the principal mass transport at times above 0.15 seconds (calculated by considering $D = 2.7 \times 10\text{-}6$ cm2/s).37 Furthermore, the role of cylindrical diffusion on mass transport depends on the length of the cylinder used for the electrochemical reaction.38 Since in BE the length of the anod-ic and cathodic zones having the right polarization for carry-ing out the desired redox reaction increases with the applied electric field,39,40 the portion of the wire where the electro-chemical reaction takes place is electric field dependent. It is noteworthy that this is only true when both, oxidation and reduction reactions, are kinetically similar ($j_{ox} \approx j_{red}$, where j is defined as the current density). In this case, for any given electric field, both polarization zones are expected to behave in a similar way. Such considerations are not required for conventional electrochemistry, since the large area of the counter electrode ensures that the rate of the reaction of inter-est, occurring at the working electrode, is not limited by the corresponding opposite reaction.

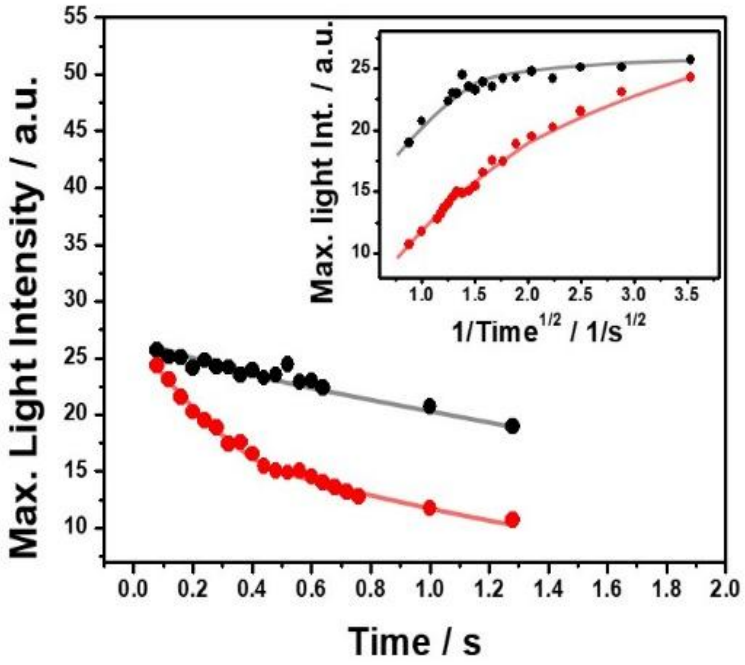

Figure 2. Maximum light emission transients obtained for a 1.91 cm bipolar LED with an uncoated (black dots) and coated cathodic arm (red dots) in a 5 mM LiClO4 solution containing a 1:1 ratio of HQ/Q (5:5 mM). The inset shows the maximum light intensity as a function of 1/t1/2.

In order to corroborate the mass transport regime, a control experiment was carried out with a BPE array where all the cathodic arms of every LED were coated with commercial nail polish, leaving only the tip exposed to the solution. Thus, each BPE mimics a classic electrochemical set-up, with the anodically polarized side (not covered) acting as the bigger counter electrode, and the much smaller cathodic tip as work-ing electrode. In this way, the reduction of Q is not limited by the corresponding oxidation of HQ, thus, charge transfer and mass transport limitations will be governed only the reduction of Q. The light emission transient obtained with such a modi-fied LED shows a response that resembles more accurately the characteristic current transients obtained by potentiostatic experiments (Figure 2, red curve). This is further illustrated by plotting the maximum light intensity as a function of 1/t-1/2, exhibiting a better linearity (r2 = 0.94) in comparison with the non-modified device (r2 = 0.59), on the same time scale (be-tween 0.4 and 1 seconds) (Figure 2, black curve).

In the next step, we tested the possibility to image the re-dox activity of a probe by using the whole BPE array, and plotting the average light intensity distribution as a function of the theoretical polarization potential difference ΔVtheo, calculated for a given electric field, in this case 1.5 V/cm (Figure 3, black dots). This plot shows a sigmoidal response, similar to a characteristic linear sweep voltammetry response obtained by conventional electrochemistry. In order to direct-ly compare the recorded light-based voltammogram with a conventional linear potentiodynamic measurement, a classic three-electrode experiment was carried out and the results were superimposed (Figure 3a, blue curve). This allows ex-pressing the light intensity distribution in terms of conven-tional potential values (E vs Ag/AgCl). As previously estab-lished by Crooks et al., the voltammogram reconstructed from the light emission intensity is plotted versus the polarization potential difference, instead of the applied potential (given versus a normal reference electrode).24

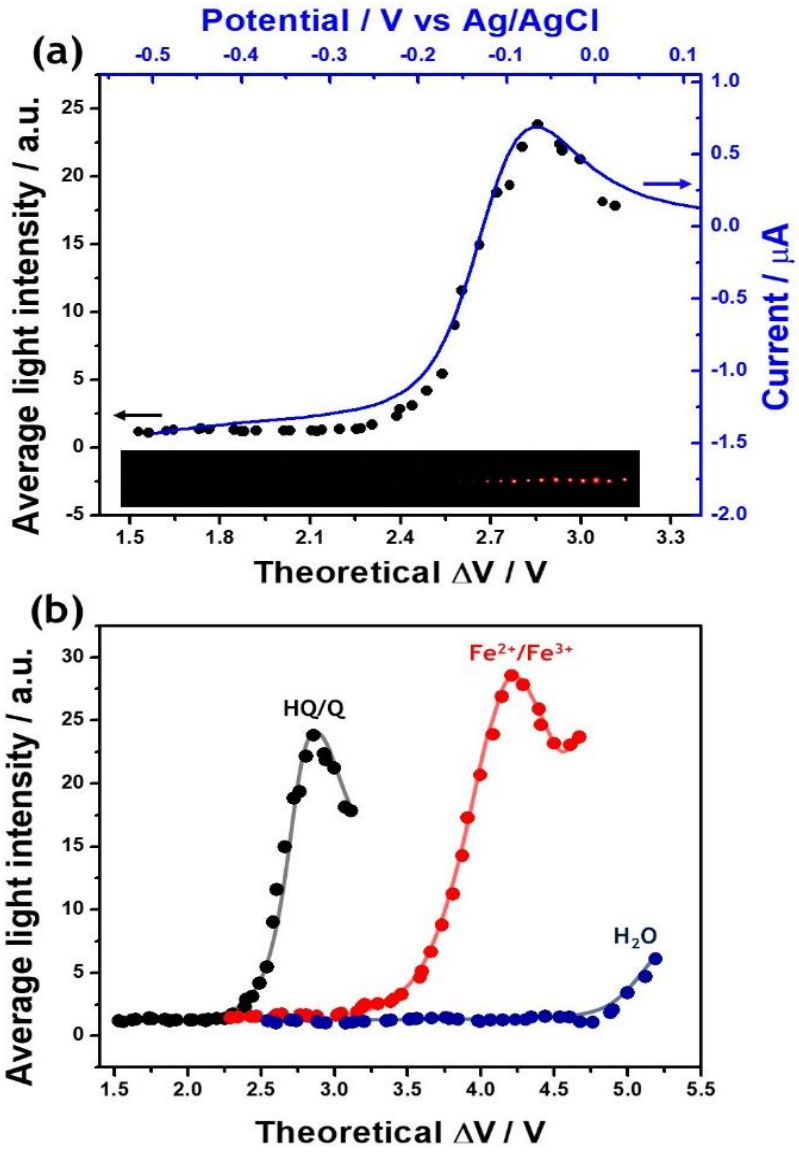

Figure 3. (a) Average of the light intensity distribution as a function of polarization potential difference experienced by the BPEs having different lengths (left axis, black dots) obtained in a 5 mM LiClO4 solution in the presence of a 1:1 ratio of HQ/Q (5:5 mM) at a constant applied electric field (1.5 V/cm), com-pared with a potentiodynamic measurement (right axis, blue line) obtained by using a classic three-electrode system. The inset shows the corresponding picture of the light-emitting BPE array. (b) Average of the light intensity distribution as a func-tion of the polarization potential difference experienced by the BPEs having different lengths obtained in a 5 mM LiClO4 solu-tion in the presence of a 1:1 ratio of HQ/Q (5:5 mM, black dots), a 1:1 ratio Fe(CN)64–/Fe(CN)63– (5:5 mM, red dots) and in the absence of redox probe (blue dots), at a constant applied electric field of 1.5, 2.25 and 2.5 V/cm, respectively. The light intensity was measured 0.4 sec after applying the potential steps. The average of the relative standard deviation from three independent experiments is ±10-15%.

Finally, in order to verify that the proposed methodology is not limited to the analysis of a single redox system, we ex-plored the possibility of imaging another electroactive probe i.e., the Fe(CN)64–/Fe(CN)63– couple. The potentiodynamic behavior of this redox system shows a slightly larger peak-to-peak separation (220 mV), in comparison with the HQ/Q pair (110 mV, Figure S2). In addition, the E1/2 value (0.11 V vs Ag/AgCl) is 240 mV more anodic than the one for the HQ/Q pair. Thus, a higher

threshold potential value to trigger the light emission is predicted for this FeII/FeIII system. Indeed, an electric field of 2.25 V/cm is required to observe the sigmoidal light intensity variation as a function of the position of the BPEs along the array. By superimposing the average light intensity distribution as a function of ΔVtheo for both redox probes, it is possible to identify unambiguously both electroac-tive systems with a difference in their respective polarization potential peaks of 1.35 V (Figure 3b). Furthermore, this meth-odology allows also the analysis of redox couples with a larger potential difference between the oxidation and reduction such as water splitting (> 1.5 V). In this case, an electric field of 2.5 V/cm is required to trigger light emission. This confirms the electroanalytical discrimination of redox systems due to their intrinsic difference in thermodynamic potential between the anodic and cathodic reactions. In addition, and most importantly, the proposed light-emitting system enables an opto-electrochemical discrimination of different analytes, without the need of adding other reagents to the solution, thus avoiding eventual interferences due to parasitic reactions.

CONCLUSIONS

In summary, we have designed a novel analytical BE setup based on an array of light-emitting bipolar electrodes, using modified LEDs with a gradually changing length. Such an array enables a lateral variation of the driving forces experi-enced by each individual BPE. It was observed that light emission occurs when the polarization potential difference ΔV is higher than the thermodynamic threshold potential. As expected, redox couples such as HQ/Q and Fe(CN)64–/Fe(CN)63– require a lower driving force to trigger light emis-sion compared to water, allowing a differentiation of redox systems due to their intrinsic difference in thermodynamic threshold potential. Most importantly, when correlating the average light intensity with the length of the BPE, and thus the driving force, the typical exponential signal increase asso-ciated with charge transfer limitations (Butler-Volmer regime) can be recorded by simply taking a single optical snapshot. Interestingly, when covering the surface of the cathodically polarized extremity of a bipolar LED and exposing only the tip to ensure that the charge transfer and mass transport at the cathode is not limited by the corresponding oxidation at the anodically polarized side, we observe a light emission transi-ent that reflects accurately the characteristic current transients obtained by potentiostatic experiments (Cottrell behavior). In addition, when plotting the average light intensity distribution of the whole LED array as a function of the theoretical polari-zation potential difference, the results are remarkably similar to characteristic linear sweep voltammetry curves obtained by conventional electrochemistry. It is important to highlight that the proposed approach already presents all the usual intrinsic advantages of bipolar electrochemistry, like for example its wireless nature, but an additional main advantage of the light-emitting electrode array is the straightforward readout of chemical information via a single snapshot experiment for which scanning of the potential is not necessary. This means that no specific and sometimes expensive equipment, such as a potentiostat, is necessary. Only a simple power supply, or in the extreme case even a classic battery, is needed, as long as its voltage is sufficient to polarize the bipolar electrodes. This enables a very simple and fast optical acquisition of infor-mation about a redox couple, in comparison with classic elec-trochemical systems, with the further advantage that no addi-tional chemicals are necessary, like for other opto-electrochemical readout schemes.

EXPERIMENTAL SECTION

Chemicals and Materials

LiClO4 (Aldrich, 99%), Hydroquinone (Aldrich, ≥ 99.5%), p-Benzoquinone (Aldrich, ≥ 98%), K3Fe(CN)6 (Aldrich, 98%), K4Fe(CN)6 3H2O (Aldrich, 98%), Au wires (d = 0.25 mm, Alfa Aesar, 99.9%), agar silver

paint (Agar scientific Ltd.) and miniaturized red light-emitting diodes (0603 SMD diode, Wurth Elektronik, 1.60 mm x 0.8 mm) were used as received. All solutions were prepared with deionized water (MilliQ Direct-Q®). Potentiodynamic experiments were per-formed with a PalmSense4 potentiostat connected to a per-sonal computer. The working electrode was a 0.25 mm diame-ter Au wire, Pt and Ag/AgCl were used as the counter and reference electrodes, respectively. For the bipolar electrochem-istry measurements, the light-emitting bipolar array was fixed at the center of a bipolar cell. Two graphite feeder electrodes were positioned at the extremities of the cell at a distance of 4 cm. The average light intensity of a single LED was calculated by following the moving average approach. The maximum light intensity of a selected LED was averaged with the light intensity of the neighboring LEDs and then for the next LED the average was moved one LED further. We calculated this average intensity in order to smoothen the eventually occur-ring arbitrary fluctuations and the better visualize the overall trend of the signal obtained by the snapshot. Experiments were monitored by using a CCD camera (CANON EOS 70D, Objective Canon Macro Lens 100 mm 1:2.8). Images were processed with Image J software. The maximum light intensi-ty of each LED was evaluated within a constant region of interest (ROI, 1500 x 90 pixels).

ASSOCIATED CONTENT

Supporting Information

The Supporting Information is available free of charge on the ACS Publications website.

Theoretical polarization potential difference as function of the BPE length, potentiodynamic experiments, light intensity distri-bution, light emission transients. (PDF)

AUTHOR INFORMATION

Corresponding Author

*E-mail: gerardo.salinassanchez@enscbp.fr, kuhn@enscbp.fr

Author Contributions

The manuscript was written through contributions of all authors

Notes

The authors declare no competing financial interest.

ACKNOWLEDGMENT

This work has been funded by the European Research Council (ERC) under the European Union's Horizon 2020 research and innovation program (grant agreement no 741251, ERC Ad-vanced grant ELECTRA).

REFERENCES

(1). Bard, A. J.; Faulker, L. R. Electrochemical Methods, 2nd ed.; Wiley: New York, 2001.

(2). Fosdick, S. E.; Knust, K. N.; Scida, K.; Crooks, R. M. Bipolar electrochemistry. Angew. Chem. Int. Ed. 2013, 52, 10438-10456.

(3) Koefoed, L.; Pedersen, S. U.; Daasbjerg, K. Bipolar electro-chemistry-A wireless approach for electrode reactions. Curr. Opin. Electrochem. 2017, 2, 13-17.

(4) Karimian, N.; Hashemi, P.; Afkhami, A.; Bagheri, H. The principles of bipolar electrochemistry and its electroanalysis applica-tions. Curr. Opin. Electrochem. 2019, 17, 30-37.

(5) Salinas, G.; Arnaboldi, S.; Bouffier, L.; Kuhn, A. Recent ad-vances in bipolar electrochemistry with conducting polymers. ChemE-lectroChem 2022, 9, e202101234.

(6) Shida, N.; Zhou, Y.; Inagi, S. Bipolar electrochemistry: A powerful tool for electrifying functional material synthesis. Acc. Chem. Res. 2019, 52, 2598-2608.

(7) Loget, G.; Li, G.; Fabre, B. Logic gates operated by bipolar photoelectrochemical water splitting. Chem. Commun. 2015, 51, 11115-11118.

(8) Anand, R. K.; Johnson, E. S.; Chiu, D. T. Negative dielectro-phoretic capture and repulsion of single cells at a bipolar electrode: the impact of faradaic ion enrichment and depletion. J. Am. Chem. Soc. 2015, 137, 776-783.

(9) Rahan, K. L.; Anand, R. K. Recent advancements in bipolar electrochemical methods of analysis. Anal. Chem. 2021, 93, 103-123

(10) Bouffier, L.; Zigah, D.; Sojic, N.; Kuhn, A. Bipolar (Bio)electroanalysis. Annu. Rev. Anal. Chem. 2021, 14, 65-86.

(11) Li, M.; Liu, S.; Jiang, Y.; Wang, W. Visualizing the zero-potential line of bipolar electrodes with arbitrary geometry. Anal. Chem. 2018, 90, 6390-6396.

(12) Villani, E.; Inagi, S. Mapping the distribution of potential gradient in bipolar electrochemical systems through luminol electro-chemiluminescence imaging. Anal. Chem. 2021, 93, 8152-8160.

(13) Oja, S. M.; Zhang, B. Imaging transient formation of diffu-sion layers with fluorescence-enabled electrochemical microscopy. Anal. Chem. 2014, 86, 12299-12307.

(14) Fosdick, S. E.; Crooks, R. M. Bipolar electrodes for rapid screening of electrocatalysts. J. Am. Chem. Soc. 2012, 134, 863-866.

(15) Zhan, W.; Alvarez, J.; Crooks, R. M. Electrochemical sensing in microfluidic systems using electrogenerated chemiluminescence as a photonic reporter of redox reactions. J. Am. Chem. Soc. 2002, 124, 13265-13270.

(16) Eßmann, V.; Santos, C. S.; Tarnev, T.; Bertotti, M.; Schuhmann, W. Scanning bipolar electrochemical microscopy. Anal. Chem. 2018, 90, 6267-6274.

(17) Bouffier, L.; Doneux, T.; Goudeau, B.; Kuhn, A. Imaging re-dox activity at bipolar electrodes by indirect fluorescence modulation. Anal. Chem. 2014, 86, 3708-3711.

(18) Eden, A.; Scida, K.; Arroyo-Curras, N.; Eijkel, J. C. T.; Meinhart, C. D.; Pennathur, S. Discharging behavior of confined bipolar electrodes: Coupled electrokinetic and electrochemical dynam-ics. Electrochim. Acta 2020, 330, 135275.

(19) Zhang, J. D.; Lu, L.; Zhu, X. F.; Zhang, L. J.; Yun, S.; Duanmu, C. S.; He, L. Direct observation of oxidation reaction via closed bipolar electrode-anodic electrochemiluminescence protocol: structural property and sensing applications. ACS Sens. 2018, 3, 2351-2358.

(20) Oja, S. M.; Zhang, B. Electrogenerated chemiluminescence reporting on closed bipolar microelectrodes and the influence of electrode size. ChemElectroChem 2016, 3, 457-464.

(21) Liu, R.; Zhang, C.; Liu, M. Open bipolar electrode-electrochemiluminescence imaging sensing using paper-based micro-fluidics. Sens. Actuators B Chem. 2015, 216, 255-262.

(22) Mavré, F.; Chow, K. F.; Sheridan, E.; Chang, B. Y.; Crooks, J. A.; Crooks, R. M. A theoretical and experimental framework for understanding electrogenerated chemiluminescence (ECL) emission at bipolar electrodes. Anal. Chem. 2009, 81, 6218-6225.

(23) Rahn, K. L.; Rhoades, T. D.; Anand, R. K. Alternating current voltammetry at a bipolar electrode with smartphone luminescence imaging for point-of-need sensing. ChemElectroChem 2020, 7, 1172-1181.

(24) Chang, B. Y.; Mavré, F.; Chow, K. F.; Crooks, J. A.; Crooks, R. M. Snapshot voltammetry using a triangular bipolar microelec-trode. Anal. Chem. 2010, 82, 5317-5322.

(25) Borchers, J. S.; Riusech, O.; Rasmussen, E.; Anand, R. K. Visual voltammogram at an array of closed bipolar electrodes in a ladder configuration. J. Anal. Test. 2019, 3, 150-159.

(26) Salinas, G.; Dauphin, A. L.; Colin, C.; Villani, E.; Arbault, S.; Bouffier, L.; Kuhn, A. Chemo-and magnetotaxis of self-propelled light-emitting chemo-electronic swimmers. Angew. Chem. Int. Ed. 2020, 59, 7508-7513.

(27) Salinas, G.; Pavel, I. A.; Sojic, N.; Kuhn, A. Electrochemis-try-based light-emitting mobile systems. ChemElectroChem, 2020, 7, 4853-4862.

(28) Sharma, R.; Velev, O. D. Remote steering of self-propelling microcircuits by modulated electric field. Adv. Funct. Mater. 2015, 25, 5512-5519.

(29) Chang, S. T.; Paunov, V. N.; Petsev, D. N.; Velev, O. D. Remotely powered self-propelling particles and micropumps based on miniature diodes. Nat. Mat. 2007, 6, 235-240.

(30) Roche, J.; Carrara, S.; Sanchez, J.; Lannelongue, J.; Loget, G.; Bouffier, L.; Fischer, P.; Kuhn, A. Wireless powering of e -swimmers Sci. Rep. 2015, 4, 6705

(31) Gupta, B.; Alfonso, M. C.; Zhang, L.; Ayela, C.; Garrigue, P.; Goudeau, B.; Kuhn, A. Wireless coupling of conducting polymer actuators with light emission. ChemPhysChem 2019, 20, 941-945.

(32) Dauphin, A. L.; Arbault, S.; Kuhn, A.; Sojic, N.; Bouffier, L. Remote actuation of a light-emitting device based on magnetic stirring and wireless electrochemistry. ChemPhysChem 2020, 21, 600-604.

(33) Zhang, X.; Chen, C.; Yin, J.; Han, Y.; Li, J.; Wang, E. Porta-ble and visual electrochemical sensor based on the bipolar light emit-ting diode electrode. Anal. Chem. 2015, 87, 4612-4616

(34) Salinas, G.; Arnaboldi, S.; Bonetti, G.; Cirilli, R.; Benincori, T.; Kuhn, A. Hybrid light-emitting devices for the straightforward readout of chiral information. Chirality 2021, 33, 875-882.

(35) Salinas, G.; Bonetti, G.; Cirilli, R.; Benincori, T.; Kuhn, A.; Arnaboldi, S. Wireless light-emitting device for the determination of chirality in real samples. Electrochim. Acta 2022, 421, 140494.

(36) Le, H.; Compton, R. G. Comparative chronoamperometry: Spheres, discs, cylinders and bands. J. Electroanal. Chem. 2020, 866, 114149.

(37) Jakobs, R. C. M.; Janssen, L. J. J.; Barendrech, E. Hydroqui-none oxidation and p-benzoquinone reduction at polypyrrole and poly-N-methylpyrrole electrodes. Electrochim. Acta 1985, 30, 1313-1321.

(38) Le, H.; Kätelhön, E.; Compton, R. G. Characterising the na-ture of diffusion via a new indicator: Microcylinder and microring electrodes. J. Electroanal. Chem. 2019, 855, 113602.

(39) Duval, J. F. L.; Minor, M.; Cecilia, J.; van Leeuwen, H. P. Coupling of lateral electric field and transversal faradaic processes at the conductor/electrolyte solution interface. J. Phys. Chem. B 2003, 107, 4143-4155

(40) Duval, J. F. L.; Buffle, J.; van Leeuwen, H. P. Quasi-reversible faradaic depolarization processes in the electrokinetics of the metal/solution interface. J. Phys. Chem. B 2006, 110, 6081-6094.

Authors are required to submit a graphic entry for the Table of Contents (TOC) that, in conjunction with the manu-script title, should give the reader a representative idea of one of the following: A key structure, reaction, equation, concept, or theorem, etc., that is discussed in the manuscript. Consult the journal's Instructions for Authors for TOC graphic specifications.